Research in Astron. Astrophys. **2011** Vol. **11** No. **10**, 1143–1157
http://www.raa-journal.org *http://www.iop.org/journals/raa*

***R**esearch in*
***A**stronomy and*
***A**strophysics*

Characteristics of convection and overshooting in RGB and AGB stars *

Xiang-Jun Lai[1,2,3] and Yan Li[1,2]

[1] National Astronomical Observatories / Yunnan Observatory, Chinese Academy of Sciences, Kunming 650011, China; *lxj@mail.ynao.ac.cn, ly@ynao.ac.cn*
[2] Key Laboratory for the Structure and Evolution of Celestial Objects, Chinese Academy of Sciences, Kunming 650011, China
[3] Graduate University of Chinese Academy of Sciences, Beijing 100049, China.

Received 2011 January 24; accepted 2011 May 23

Abstract Based on the turbulent convection model (TCM) of Li & Yang, we have studied the characteristics of turbulent convection in the envelopes of 2 and $5M_{\odot}$ stars at the red giant branch and asymptotic giant branch phases. The TCM has been successfully applied over the entire convective envelopes, including the convective unstable zone and the overshooting regions. We find that the convective motions become progressively stronger when the stellar models are located farther up along the Hayashi line. In the convective unstable zone, we find that the turbulent correlations are proportional to functions of a common factor $(\nabla - \nabla_{\rm ad})\overline{T}$, which explains similar distributions in those correlations. For the TCM we find that if the obtained stellar temperature structure is close to that of the mixing length theory (MLT), the convective motion will have a much larger velocity and thus be more violent. However, if the turbulent velocity is adjusted to be close to that of the MLT, the superadiabatic convection zone would be much more extended inward, which would lead to a lower effective temperature of the stellar model. For the overshooting distance, we find that the e-folding lengths of the turbulent kinetic energy k in both the top and bottom overshooting regions decrease as the stellar model is progressively located farther up along the Hayashi line, but both the extents of the decrease are not obvious. The overshooting distances of the turbulent correlation $\overline{u_r' T'}$ are almost the same for the different stellar models with the same set of TCM parameters. For the decay modes of the kinetic energy k, we find that they are very similar for different stellar models based on the same set of TCM parameters, and there is a nearly linear relationship between $\lg k$ and $\ln P$ for different stellar models. When $C_{\rm s}$ or α increases while the other parameters are fixed, the obtained linearly decaying distance will become longer.

Key words: stars: RGB and AGB — convection of stars — turbulent convection model: convective overshooting

∗ Supported by the National Natural Science Foundation of China.

1 INTRODUCTION

Red giant branch (RGB) and asymptotic giant branch (AGB) stars are characterized by the convective motion in their envelopes, which can extend over an enormous range in mass (or radius). Because of the huge scale of convection zones and the small viscosity of the stellar material, turbulent instead of laminar flow always occurs in their outer envelopes. Turbulent convection may result in many important effects in stars: mixing different elements to be homogeneous in the convection zone and adding fresh fuel to the nuclear burning region, dredging the internal material processed by H or He burning up to the stellar surface and acting as an important means for heat transfer. These effects significantly influence the structure and evolution of stars. Many observational phenomena appearing in the RGB and AGB stars are ascribed to the convection.

For the RGB stars as an example, many of them show chemical anomalies (Pilachowski et al. 1993; Charbonnel 1995; Gratton et al. 2000, 2004; Kraft et al. 1993; Ramírez & Cohen 2002; Busso et al. 2007; Recio-Blanco & de Laverny 2007). We are still perplexed by the so-called carbon star mystery (Iben 1981, 1975, 1977; Sackmann 1980; Lattanzio 1989; Hollowell & Iben 1988; Straniero et al. 1997; Herwig et al. 1997; Herwig 2005) for AGB stars. Furthermore, the observed mass loss occurring in the RGB and AGB stars may be due to the turbulent pressure (Jiang & Huang 1997). To solve these problems, we first need to accurately deal with the convection model and to learn details of characteristics of the convective motion.

For some RGB and AGB stars the convective motion near the surface of the stellar envelope is superadiabtic because of less efficient convective energy transport, and may sometimes become supersonic based on the mixing-length theory (MLT) (Deng & Xiong 2001). The MLT (Vitense 1953; Böhm-Vitense 1958) is commonly used to deal with the convection. However, due to its simplicity, many shortcomings are found (Renzini 1987; Baker & Kuhfuss 1987; Spruit et al. 1990; Pedersen et al. 1990), which thus lead to some confusing and debatable problems, for example, convective overshooting (e.g. Saslaw & Schwarzschild 1965), semiconvection (e.g. Castellani et al. 1971; Sreenivasan & Wilson 1978) and breathing convection (e.g. Castellani et al. 1985). Therefore, new convection models have been proposed, for example, non-local mixing length theories (Ulrich 1970; Maeder 1975; Bressan et al. 1981) and full-spectrum convection theory (Canuto & Mazzitelli 1991Canuto & Mazzitelli 1991). However, they are still based on the framework of the MLT. A better theory to overcome the MLT's drawbacks is the turbulent convection models (TCMs), which are deduced directly from the Navier-Stokes equations, and can describe many of the turbulence properties (Xiong 1979, 1981, 1985, 1990; Canuto 1992, 1994, 1997; Xiong et al. 1997; Canuto & Dubovikov 1998; Canuto et al. 1996). However, the dynamic equations for turbulent correlations are expressed by higher order correlations due to the inherent non-linearity of the Navier-Stokes equations.

Therefore, these equations need to be truncated with some closure approximations in order to be applicable in calculations of the associated stellar structure and evolution. Nevertheless, some free parameters have to be introduced by the closure assumptions. Different closure assumptions correspond to different TCMs, and many of them may not be easily incorporated into stellar evolution code. Recently, a simple TCM proposed by Li & Yang (2007) was successfully applied to the solar models (Yang & Li 2007), in which the introduced parameters of the TCM are directly related to the corresponding turbulence physics. Some significant changes in the structure of the solar convection zone and better results, compared to the solar p-mode observations, were obtained. Shortly afterwards, Zhang & Li (2009) successfully applied the new model to the overshooting region of the solar convection zone.

Up to now, the TCMs have seldom been applied to very large convective envelopes of stars, e.g. in the RGB or AGB stars, which are rather different from the solar environment. Furthermore, in view of the key roles that convection played in these stars, we choose three sites of stellar evolution to test the TCM of Li & Yang (2007). We try to discover convection characteristics for two stars of 5 and $2M_{\odot}$ at the RGB and AGB phases, and to find out their dependence on the TCM's parameter. To

analyze the properties of the turbulent correlations among velocity and temperature fluctuations, we separate the whole convection envelope (derived self-consistently from the TCM) into the convective unstable zone and the convective overshooting regions, respectively. We firstly describe the basic equations of the TCM in Section 2. The information about the evolutionary code and input physics are described in Section 3. In Section 4, the convection characteristics in the convective unstable zone and overshooting regions are presented and discussed, respectively. The dependence of the structure of the overshooting regions on the TCM's parameters is given in Section 5. Finally, some concluding remarks are summarized in Section 6.

2 EQUATIONS OF TCM

Using the Reynolds decomposition approximation, and with the aid of some closure approximations, the second-order moment equations of the TCM are (see Li & Yang 2007 for details)

$$\frac{1}{\overline{\rho}r^2}\frac{\partial}{\partial \ln \overline{P}}\left(C_{\rm s}\overline{\rho}r^2\frac{\overline{u_r'u_r'}}{\sqrt{k}}\frac{\partial \overline{u_r'u_r'}}{\partial \ln \overline{P}}\right)=C_k\frac{\sqrt{k}}{\alpha}\left(\overline{u_r'u_r'}-\frac{2}{3}k\right)+\frac{2}{3}\frac{k^{3/2}}{\alpha}+\frac{2\beta g_r}{\overline{T}}H_P\overline{u_r'T'}, \quad (1)$$

$$\frac{1}{\overline{\rho}r^2}\frac{\partial}{\partial \ln \overline{P}}\left(C_{\rm s}\overline{\rho}r^2\frac{\overline{u_r'u_r'}}{\sqrt{k}}\frac{\partial k}{\partial \ln \overline{P}}\right)=\frac{k^{3/2}}{\alpha}+\frac{\beta g_r}{\overline{T}}H_P\overline{u_r'T'}, \quad (2)$$

$$\frac{2}{\overline{\rho}r^2}\frac{\partial}{\partial \ln \overline{P}}\left(C_{t1}\overline{\rho}r^2\frac{\overline{u_r'u_r'}}{\sqrt{k}}\frac{\partial \overline{u_r'T'}}{\partial \ln \overline{P}}\right)=\left[\frac{\overline{\rho}c_pH_P}{\lambda}\overline{u_r'T'}-\overline{T}(\nabla_R-\nabla ad)\right]\overline{u_r'u_r'}$$
$$+\frac{\beta g_r}{\overline{T}}H_P\overline{T'^2}+C_t\left(\frac{\sqrt{k}}{\alpha}+\frac{\lambda}{\overline{\rho}c_p\alpha^2H_P}\frac{\varepsilon^2}{k^3}\right)\overline{u_r'T'}, \quad (3)$$

$$\frac{1}{\overline{\rho}r^2}\frac{\partial}{\partial \ln \overline{P}}\left(C_{e1}\overline{\rho}r^2\frac{\overline{u_r'u_r'}}{\sqrt{k}}\frac{\partial \overline{T'^2}}{\partial \ln \overline{P}}\right)=2\left[\frac{\overline{\rho}c_pH_P}{\lambda}\overline{u_r'T'}-\overline{T}(\nabla_R-\nabla ad)\right]\overline{u_r'T'}$$
$$+2C_e\left(\frac{\sqrt{k}}{\alpha}+\frac{\lambda}{\overline{\rho}c_p\alpha^2H_P}\right)\overline{T'^2}. \quad (4)$$

The terms on the left-hand side of Equations (1)–(4) describe diffusion process of the turbulence, representing the non-local characteristics of turbulence and mainly describing the properties of the overshooting regions outside the Schwarzschild boundaries of a convection zone. The terms on the right-hand side of Equations (1)–(4) represent some production and dissipation behavior of the turbulence. All the symbols appearing in the above equations have their usual meaning (Li & Yang 2001, 2007). There are seven free parameters in the above equations. They are C_t, C_e, C_k, C_{t1}, C_{e1}, $C_{\rm s}$, and α. The former three ones are dissipation parameters which describe respectively the dissipation of the turbulent correlation $\overline{u_r'T'}$, the dissipation of the temperature fluctuation $\overline{T'^2}$ and the anisotropic degree of the turbulence. The larger their values are, the smaller the convective heat fluxes will be (Li & Yang 2007). The next three parameters measure the extent of diffusion related respectively to the three turbulent correlations $\overline{u_r'T'}$, $\overline{T'^2}$ and $\overline{u_r'u_r'}$. Larger values of them will result in lowered and expanded profiles of these correlations (Li & Yang 2007). The last parameter α, the ratio of a typical length l to the local pressure scaleheight, is introduced by the closure assumption similar to the mixing length parameter in the MLT. The effects of these parameters on the properties of turbulence and on the structure of the solar convection zone are investigated by Li & Yang (2007) and Zhang & Li (2009). Here we choose several sets of these parameters' values to study the properties of the turbulent convection in the RGB and AGB stars.

3 INPUT PHYSICS

We calculate the evolution of two stars of 2 and $5M_\odot$ respectively. The initial composition ($Z = 0.02$, $X = 0.7$) is fixed for both stellar models.

Table 1 Information of the TCM's Parameters

Model Name	C_t	C_e	C_k	C_{t1}	C_{e1}	$C_{\rm s}$	α
MLT							1.70
LM	3.0	1.25	2.5				0.90
NLMa	3.0	1.25	2.5	0.03	0.03	0.03	0.90
NLMb1	7.0	0.20	2.5	1.0×10^{-7}	1.0×10^{-7}	0.10	0.76
NLMb2	7.0	0.20	2.5	1.0×10^{-7}	1.0×10^{-7}	0.10	0.74
NLMb3	7.0	0.20	2.5	1.0×10^{-7}	1.0×10^{-7}	0.10	0.15
NLMc1	3.0	1.25	2.5	0.05	0.05	0.05	0.68
NLMc2	3.0	1.25	2.5	0.05	0.05	0.04	0.68
NLMc3	3.0	1.25	2.5	0.05	0.05	0.03	0.68
NLMc4	3.0	1.25	2.5	0.05	0.05	0.02	0.68
NLMc5	3.0	1.25	2.5	0.05	0.05	0.01	0.68
NLMd	0.2	0.10	2.5	0.15	0.25	0.10	0.05

The free parameters adopted in the TCM can be determined by the fluid dynamics experiments in the terrestrial environment (e.g. Hossain & Rodi 1982). Given a set of appropriate values of dissipation and diffusion parameters, the value of α can be determined by calibrating the solar model (Li & Yang 2007; Zhang & Li 2009). The value of α obtained in this way can be used for RGB or AGB calculations, but this approach sacrifices the uncertainty of its value (Herwig 2005). In this paper, we adopt several sets of the parameter values, which are derived directly from or mainly based on the works of Li & Yang (2007) and Zhang & Li (2009) for the solar model and are shown in Table 1. These values of C_t, C_e and C_k are mainly derived from the terrestrial experiments and their typical values are 3.0, 1.25 and 2.5, respectively. Nevertheless, $C_t = 7.0$ is taken from the work of Canuto (1993) and $C_t = 0.20, C_e = 0.10$ from the suggestion that smaller values of them will lead to a better result compared to the solar p-mode observation (Yang & Li 2007). Furthermore, $C_{t1} = C_{e1} = 10^{-7}$ are adopted, meaning there is a negligible diffusion effect of $\overline{u_r' T'}$, $\overline{T'^2}$ and a local convection model, to assure that almost the same temperature structure in the stellar model can be obtained for both the MLT and TCM and then a meaningful comparison between them can be made, which will be discussed in the following Section 4.3. For simplicity, we call the TCM with the diffusion terms in Equations (1)–(4) non local models (NLMs) and the TCM without the diffusion terms local models (LMs). The MLT with $\alpha = 1.70$ is also adopted to calculate the stellar convection at the RGB and AGB phases for comparisons. In Table 1, both of the parameter sets of NLMa and NLMd correspond to the standard solar model calibration.

The stellar evolution code used in the present paper was originally described by B. Paczynski and M. Kozlowski and was updated by R. Sienliewicz. Nuclear reaction rates are adopted from BP95 (Bahcall et al. 1995). The equation of state is the OPAL EOS from Rogers (1994) and Rogers et al. (1996). The OPAL opacities GN93hz series (Rogers & Iglesias 1995; Iglesias & Rogers 1996) are used in the high-temperature region. In the stellar atmosphere, low-temperature opacities from Alexander & Ferguson (1994) are used.

To study the convection properties based on the TCM, we select three evolved models during the RGB and AGB phases derived from the MLT, which are indicated by solid stars in Figure 1.

4 CHARACTERISTICS OF TURBULENCE

4.1 Profiles of the Turbulent Correlations

The profiles of the turbulent correlations $\sqrt{k}$, $\overline{u_r' T'}$ and $\overline{T'^2}$ are displayed in Figure 2 for the $5M_\odot$ model at the AGB phase. It can be seen that convection widely develops in the stellar envelope $(3.5 \leq \lg T \leq 6.4)$ and the turbulent kinetic energy k stays at a high level in most of the convection zone. In particular, there are several peaks for all the three correlations appearing at almost the same

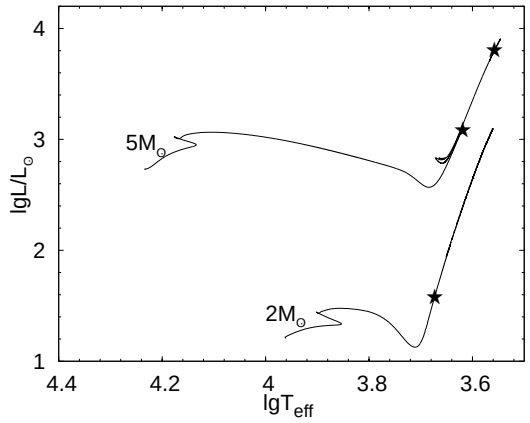

Fig. 1 HR diagram for the stellar models of 2 and $5M_\odot$ based on the MLT. The three solid stars indicate the certain locations of the stellar models during the RGB ($2M_\odot$: $\lg L/L_\odot = 1.58, T_{\rm eff} = 4750\,{\rm K}$; $5M_\odot$: $\lg L/L_\odot = 3.09, T_{\rm eff} = 4190\,{\rm K}$) and AGB ($5M_\odot$: $\lg L/L_\odot = 3.81, T_{\rm eff} = 3570\,{\rm K}$) phases.

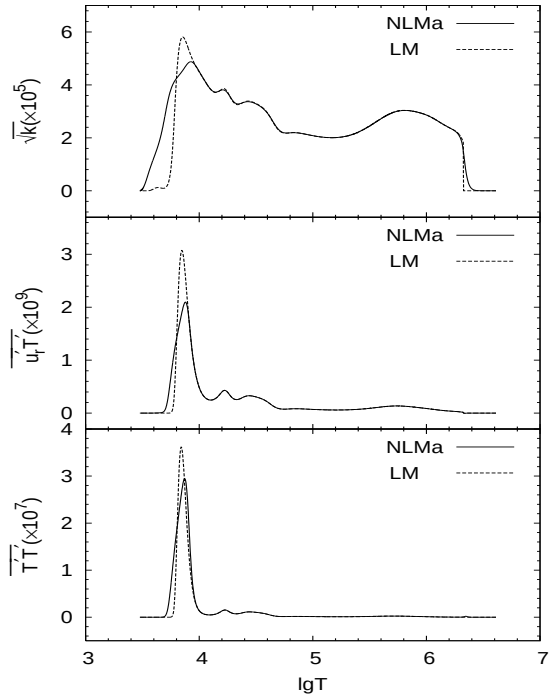

Fig. 2 Distributions of the turbulent correlations for the $5M_\odot$ star at the AGB phase. The solid lines are for NLMa, dashed lines for LM.

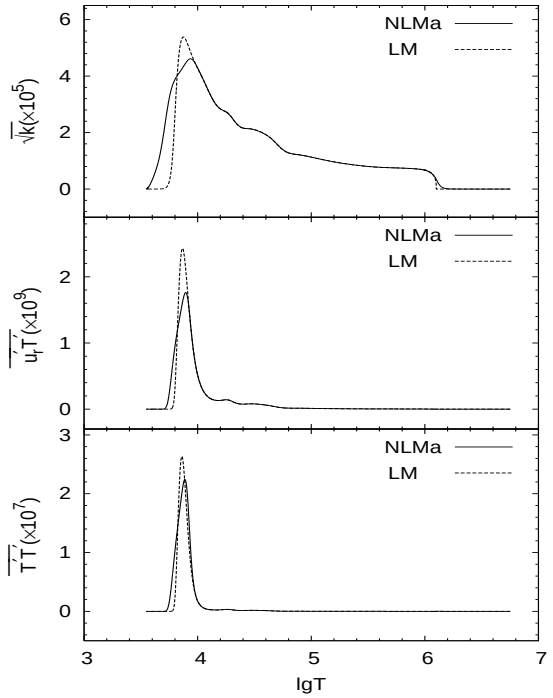

Fig. 3 Same as Fig. 2, but for the $5M_\odot$ star at the RGB phase.

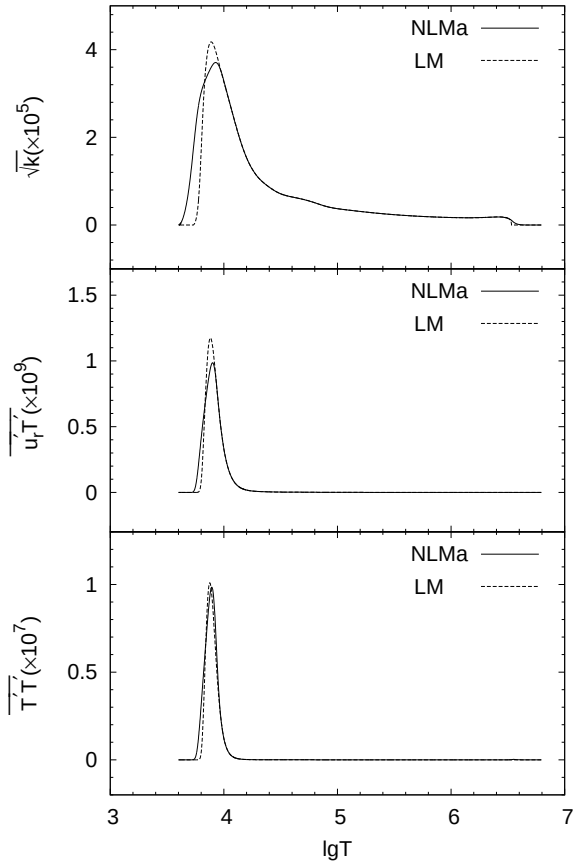

Fig. 4 Same as Fig. 2, but for the $2M_\odot$ star at the RGB phase.

locations. The appearance of the maximum turbulent kinetic energy is mainly due to ionization of hydrogen and helium which effectively blocks the transfer of heat and results in strong buoyancy to drive the convective motion. The profiles of the correlations $\overline{u_r' T'}$ and $\overline{T'^2}$ vary in a similar way as that of $\sqrt{k}$, except that the largest peaks are much higher than that of $\sqrt{k}$.

Diffusion terms in the turbulence equations are taken into account in NLMa but not in LM. As a result, the non-local effect behaves remarkably for NLMa around the boundaries of the convective unstable zone, especially around the upper boundary where the NLMa's solution significantly deviates from the LM's. However, the non-local effect can safely be ignored in the interior of the convective unstable zone because the turbulent correlations are distributed quite homogeneously there. These conclusions agree well with those of Yang & Li (2007) and Deng & Xiong (2008).

However, for the other two stellar models of 5 and $2M_\odot$ at the RGB phase, the profiles of the three correlations, which are respectively shown in Figures 3 and 4, have some differences for both NLMa and LM. These two models have smaller values for the three correlations. It means that the turbulent motion is less violent and thus transfers less heat. Furthermore, except for the maximum peak of those correlations, the other peaks become less prominent, especially for the model of $2M_\odot$ at the RGB phase. In addition, near the bottom of the convection envelope, the turbulent kinetic energy k has a weak peak, and its value seems to decrease monotonically with the stellar luminosity.

In other words, the convective motion becomes progressively stronger when the stellar models are located farther up along the Hayashi line.

4.2 Turbulence Properties in the Convective Unstable Zone

In order to understand the properties of turbulence in the convective unstable zone, some assumptions are invoked to obtain the explicit relationships between the correlations $\sqrt{k}$, $\overline{u_r'T'}$ and $\overline{T'^2}$. According to the result stated in the former section, the diffusion terms on the left hand sides of Equations (1)–(4) can be approximately ignored in the convective unstable zone. With the aid of Equations (1)–(4) we get

$$\overline{T'^2} = \frac{D(\nabla - \nabla_{\rm ad})\overline{T}^2 k - D(\nabla - \nabla_{\rm ad})\overline{T}^2 k\sqrt{1 + 4\frac{C_t}{C_e}\frac{k}{D^2\alpha^2 H_P g_r \beta(\nabla_{\rm ad} - \nabla)}}}{2H_P g_r \beta}, \tag{5}$$

where $D = \frac{4}{3C_k} + \frac{2}{3}$. In view of the mixing-length theory,

$$k = \frac{g\delta}{8H_P}(\nabla - \nabla_{\rm ad})l^2 \sim c_p \nabla_{\rm ad}(\nabla - \nabla_{\rm ad})\overline{T}. \tag{6}$$

Equation (5) can be further reduced to be

$$\overline{T'^2} \sim \frac{D\alpha^2}{8}(\nabla - \nabla_{\rm ad})^2\overline{T}^2. \tag{7}$$

By utilizing Equation (6) and Equation (2), the velocity-temperature correlation can be approximated as

$$\overline{u_r'T'} \sim \sqrt{c_p\nabla_{\rm ad}}(\nabla - \nabla_{\rm ad})^{3/2}\overline{T}^{3/2}. \tag{8}$$

It can be seen that all the three correlations depend on $(\nabla - \nabla_{\rm ad})\overline{T}$, which explains why the three correlations peak at almost the same places in the convective unstable zone.

Figure 5 shows the profiles of k, $(\overline{u_r'T'})^{2/3}$, $(\overline{T'^2})^{1/2}$ and $(\nabla - \nabla_{\rm ad})\overline{T}$ for NLMa of the $5M_\odot$ star at the AGB phase. It can be seen that the profiles of $(\overline{u_r'T'})^{2/3}$, $(\overline{T'^2})^{1/2}$ and $(\nabla - \nabla_{\rm ad})\overline{T}$ behave in a very similar way in most of the convective unstable zone. However, the profile of k deviates significantly from the others, but its overall trend is almost consistent with them. It should be noted that the above results are suitable for other stellar models.

4.3 Comparisons with the MLT

Results of two TCMs (NLMb1 and NLMb3) are compared with that of the MLT. Firstly, for the comparison between NLMb1 and the MLT in the left panel of Figure 6, we can find that the temperature gradients ∇ are almost the same, which means that NLMb1 will result in a similar stellar structure as that for the MLT in the convective unstable zone. However, the value of the turbulence velocity ($\sim \sqrt{k}$) of NLMb1 is much larger than that of the MLT. In other words, for a fixed heat flux transferred by the convective motion, a larger value of convective velocity is requested for the TCM. This is partly because the dissipation effects of the turbulent convection, measured by the parameters C_t, C_e and C_k, are fully taken into account.

When decreasing the value of parameter α, for example $\alpha = 0.15$, however, we obtain an almost equivalent profile of the convective velocity as the result of the MLT, which is shown in the right panel of Figure 6 (namely NLMb3). It can be found that the temperature gradient ∇ of NLMb3 is much larger than that of the MLT near the top of the convection envelope and extending to $\lg T \approx 4.7$ where it approaches the adiabatic temperature gradient $\nabla_{\rm ad}$, a place much deeper than the case of

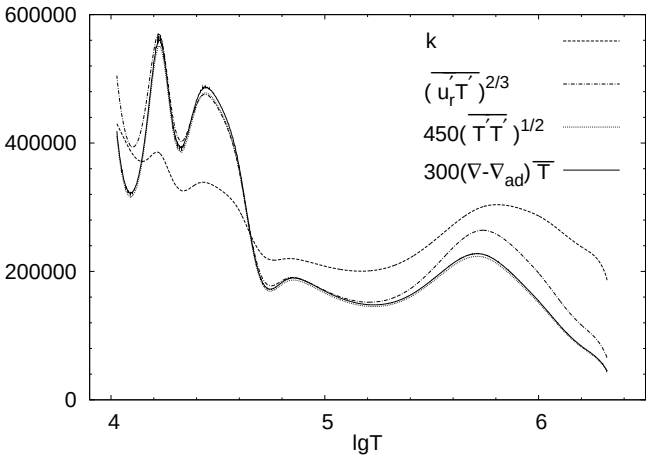

Fig. 5 Profiles of k, $(\overline{u_r'T'})^{2/3}$, $(\overline{T'^2})^{1/2}$ and $(\nabla - \nabla_{\rm ad})\overline{T}$ at the AGB phase of the $5M_\odot$ star based on NLMa.

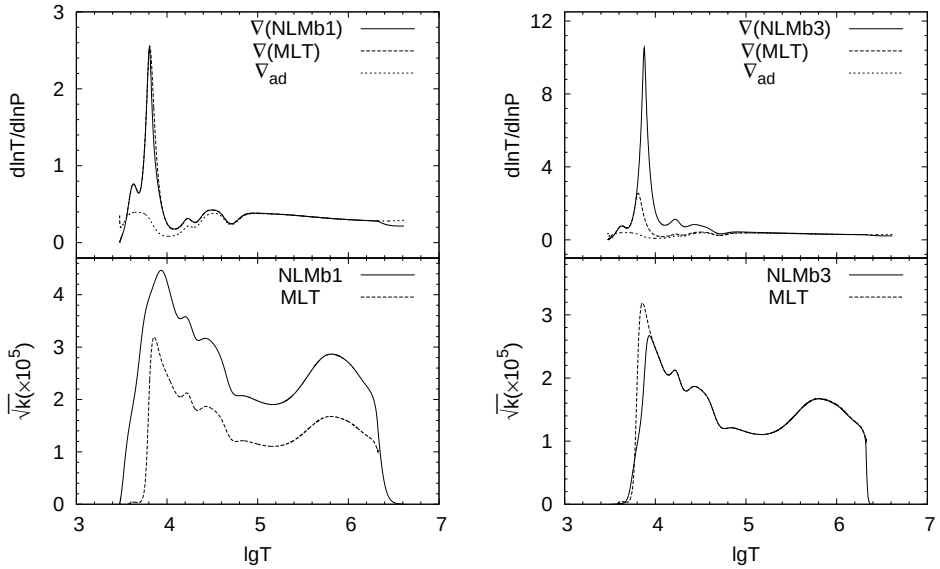

Fig. 6 Temperature gradient (including the real and adiabatic ones) and the square root of the turbulent energy $\sqrt{k}$ as functions of the temperature for the $5M_\odot$ star at the AGB phase (the same as in Fig. 2). The dashed line is for MLT, the solid lines in the left panels are for NLMb1 and the solid lines in the right panels are for NLMb3.

the MLT being approximately at $\lg T \approx 4.1$. It means that the superadiabatic convection region is much more extended inward for the TCM than the case of the MLT and the stellar models based on the TCM will have lower effective temperature than that of the MLT.

The results obtained above are mainly based on the star of $5M_\odot$ at the AGB phase. Likewise, these conclusions are still valid for the $2M_\odot$ star at the RGB phase and the $5M_\odot$ star at the RGB phase. Figure 7, as an example, shows the case of the $2M_\odot$ star at the RGB phase. It should be noted

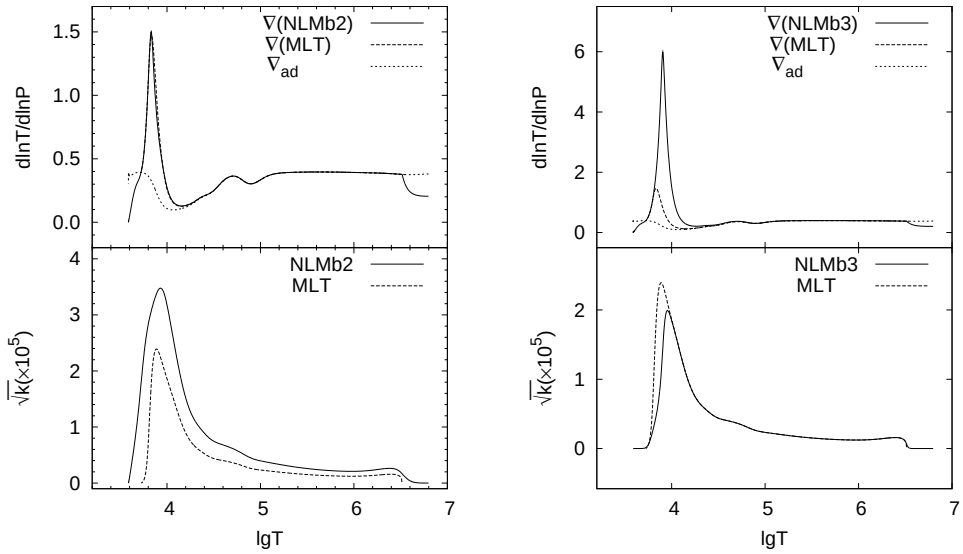

Fig. 7 Same as Fig. 6, but for the $2M_{\odot}$ star at the RGB phase.

from the right panel of Figure 7 that the superadiabatic convection region does not extend so much inward as in the case of the $5M_{\odot}$ star at the AGB phase.

4.4 Turbulence Properties in the Overshooting Region

The turbulent correlations in the top and bottom overshooting regions are shown in Figures 8–10 for the considered stellar models. It can be found that the turbulent kinetic energy k monotonically decreases outwards and tends to zero from the boundaries of the convective unstable zone into the overshooting regions. For the correlation $\overline{T'^2}$, there is a peak in both the top and bottom overshooting regions, with its value being positive and much larger than that of Zhang & Li (2009). There is an exception in the top overshooting region for the $2M_{\odot}$ star at the RGB phase seen in the left panel of Figure 10, with the peak of $\overline{T'^2}$ disappearing completely. Nevertheless, the value of the correlation $\overline{u'_r T'}$ is always negative in both the top and bottom overshooting regions. As a result, the temperature gradient ∇ is greater than the radiative temperature gradient ∇_R but smaller than the adiabatic one $\nabla_{\rm ad}$.

On the other hand, the overshooting extents are different for the different correlations in a certain overshooting region. The profile of $\sqrt{k}$ approximately demonstrates the distance that a convective cell can reach beyond the boundaries of the convective unstable zone. Its overshooting distance and decaying mode will be very important to the chemical mixing in the overshooting region, if it is used to construct the diffusion process of chemical mixing (e.g. Freytag et al. 1996; Herwig et al. 1997; Salasnich et al. 1999; Ventura & D'Antona 2005). For the three stellar models, our numerical results show that the e-folding length of $\sqrt{k}$ in the top overshooting region decreases when the stellar model is located progressively higher along the Hayashi line (they are 0.37, 0.34 and 0.34, respectively, in the units of the local pressure scale height H_P), and the case in the bottom overshooting region behaves in the same way (they are 0.24, 0.23 and 0.21 H_P, respectively), but the difference among them is not obvious in both the top and bottom overshooting regions. However, for the case of $\overline{u'_r T'}$ that can be inferred by the length of the region satisfying $\nabla_{\rm ad} > \nabla > \nabla_R$, all the overshooting distances in the bottom overshooting regions for the three models are about $0.15\,H_P$. It means that

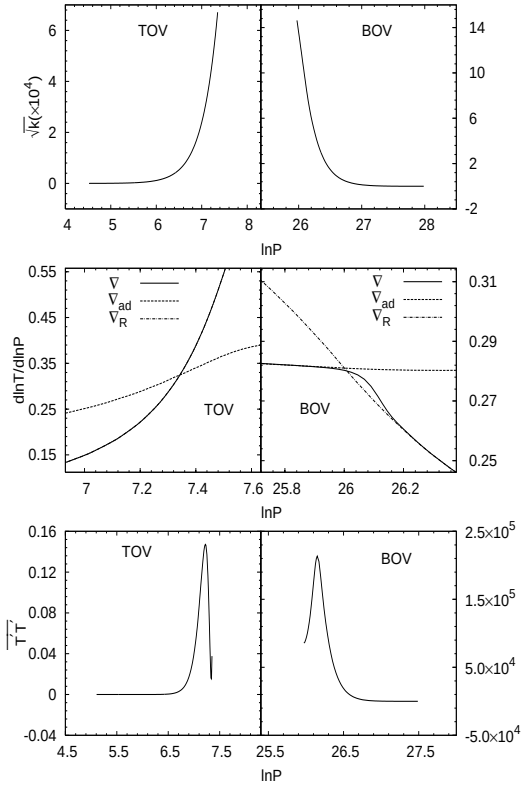

Fig. 8 Distributions of $\sqrt{k}$, $\overline{T'^2}$ and the temperature gradients in the top overshooting region and the bottom overshooting region of the $5M_\odot$ star at the AGB phase according to NLMa.

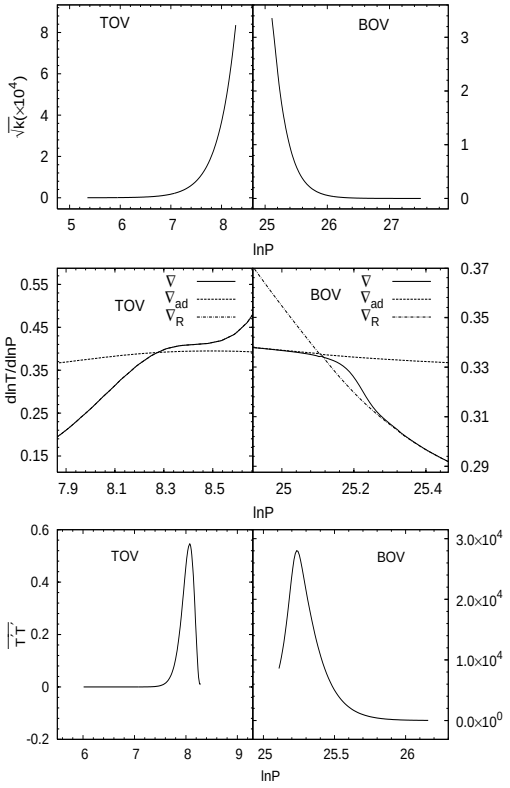

Fig. 9 Same as Fig. 8, but for the $5M_\odot$ star at the RGB phase.

the bottom convective overshooting has a similar effect on the stellar structure for all of the stellar models. In the top overshooting regions, however, it can be seen that ∇ and ∇_R nearly completely overlap each other, except for a tiny difference in the $2M_\odot$ star at the RGB phase. This may be due to very low density in the top overshooting regions, resulting in the convective heat flux being comparatively rather low.

5 DEPENDENCE OF THE STRUCTURE OF THE OVERSHOOTING REGIONS ON TCM PARAMETERS

The dependence of convection characteristics of the sun on the TCM's parameters has been extensively investigated (Li & Yang 2007; Zhang & Li 2009). The turbulent correlations are mainly affected by the corresponding dissipation and diffusion parameters. The ratio of the radial kinetic energy to the horizontal one $\overline{u'_r u'_r}/\overline{u'_h u'_h}$ is shown in Figure 11 for the AGB model of $5M_\odot$, focusing on the effect of the value of C_s on the convective structure in the overshooting regions, because C_s is the most sensitive parameter to determine the overshooting distance (Zhang & Li 2009). It can be seen that with the convective cells penetrating progressively more into the top overshooting region, the convection becomes progressively more horizontally dominated. In particular, the turbulence is isotropic when $\overline{u'_r u'_r}/\overline{u'_h u'_h} = 0.5$. It can be seen that the larger the value of C_s is, the longer the

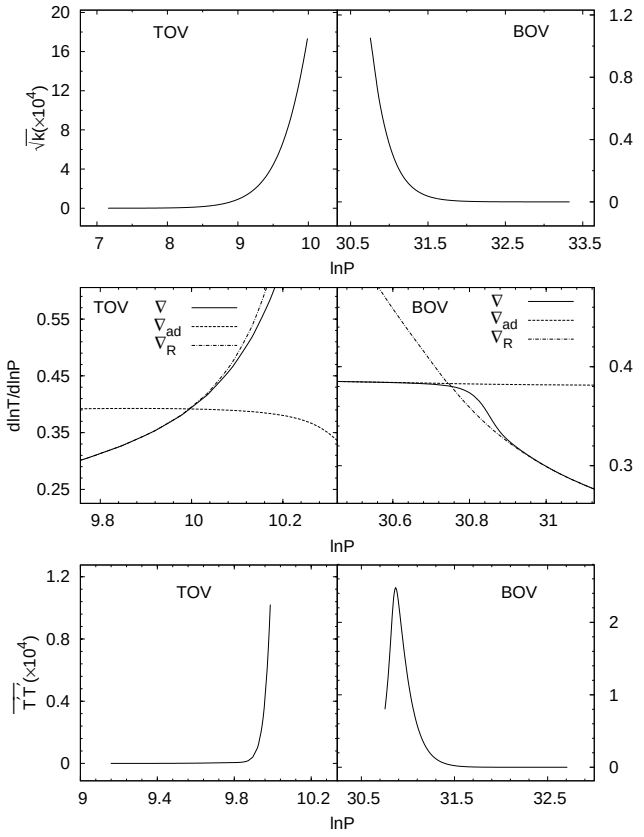

Fig. 10 Same as Fig. 8, but for the $2M_\odot$ star at the RGB phase.

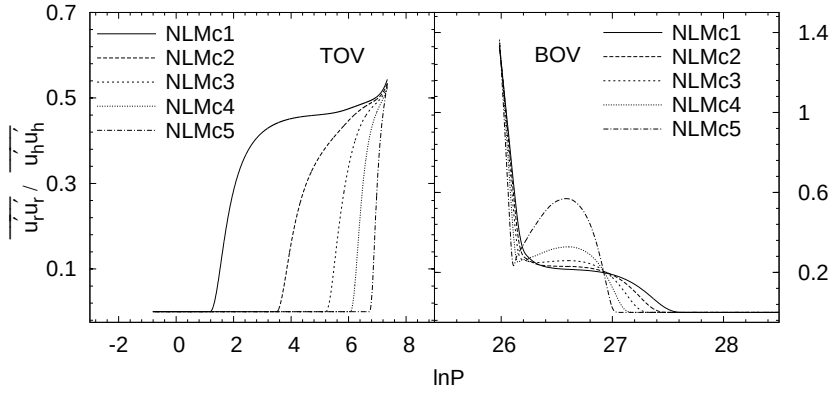

Fig. 11 Ratio of the radial turbulent kinetic energy to the horizontal one $\overline{u_r'u_r'}/\overline{u_h'u_h'}$ with different TCM parameters for the $5M_\odot$ star at the AGB phase.

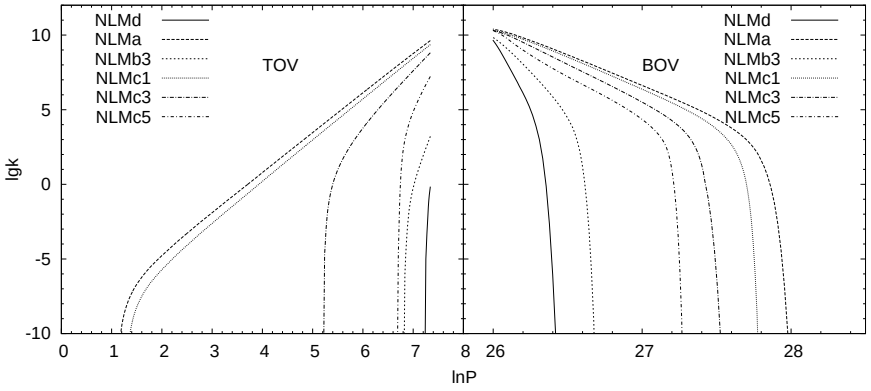

Fig. 12 Decay mode of the turbulent energy k in the top overshooting zone and the bottom overshooting zone of the $5M_{\odot}$ star at the AGB phase according to some non-local models.

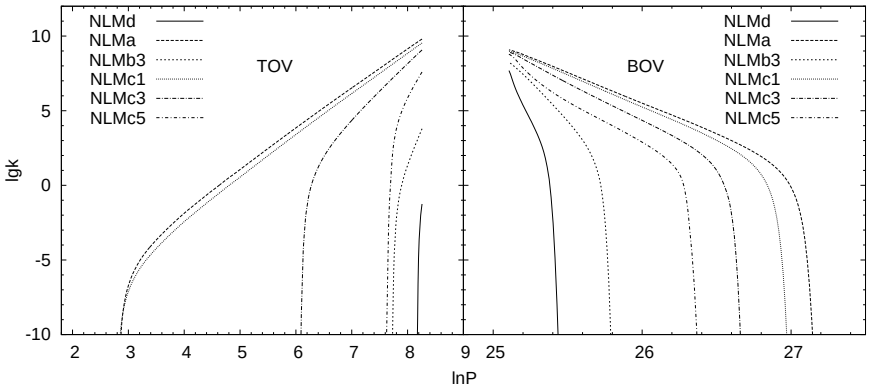

Fig. 13 Same as Fig. 12, but for the $5M_{\odot}$ star at the RGB phase.

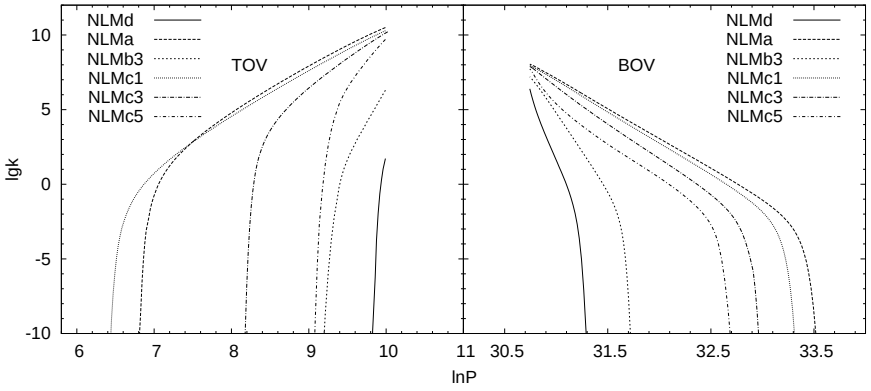

Fig. 14 Same as Fig. 12, but for the $2M_{\odot}$ star at the RGB phase.

isotropic turbulence will develop in the top overshooting region. With respect to the bottom overshooting region, the ratio $\overline{u_r'u_r'}/\overline{u_h'u_h'}$ shows a much more complicated behavior for smaller values of $C_{\rm s}$. When $C_{\rm s}$ is large enough, this complication disappears and the convection becomes progressively more horizontally dominated as the convection penetrates inward into the overshooting region.

The decaying law of the turbulent kinetic energy k is a crucial factor determining the efficiency of convective mixing in the overshooting regions. The decay modes of the turbulent kinetic energy k in the overshooting regions are given in Figures 12–14 for the three stellar models based on different choices of the TCM parameters. There is a nearly linear relation between $\lg k$ and $\ln P$ before a turning point on the curve of $\lg k$, beyond which k begins to drop promptly to zero. For example, for NLMa the relation can be approximated as $\lg k = 2.72 \ln P + C$ in the top overshooting regions, where $C = -16.8, -12.4$ and -10.2, respectively, for the three stellar models up along the Hayashi line. On the other hand, in the bottom overshooting regions we can obtain similar relations; for instance, for NLMc3 the result is $\lg k = -4.98 \ln P + C$, where $C = 161, 133.8$ and 140 for the three stellar models. It should be noted that the slope of the decaying law seems to be only a function of the TCM's parameters, and the stellar parameters only affect its constant value.

The extension of these linearly decaying regions and the slope of the decaying law are sensitive to the TCM's parameters. It can be found that when $C_{\rm s}$ increases while the other parameters are fixed (e.g. NLMc1, NLMc3, NLMc5), the turbulent kinetic energy decays progressively more slowly, and the obtained linearly decaying distance will become longer. For example, for the model of a $5M_\odot$ star at the AGB phase in Figure 12, the length of the linearly decaying distance in the bottom overshooting region for NLMc1, NLMc3 and NLMc5 are respectively about 1.2, 1.4 and 1.7 H_P. On the other hand, when the value of parameter α increases, the slope of the decaying law becomes less and the linearly decaying distance is significantly prolonged as seen by comparing the result of NLMd with that of NLMa. From Figures 12–14, it can be found that the decaying modes of k are very similar for stars of different masses and evolutionary stages with the same values of the TCM parameters.

6 CONCLUDING REMARKS

Based on the TCM of Li & Yang (2007) we have obtained the characteristics of the turbulent convection in the RGB and AGB stars with huge convection zones in their envelopes. Some sets of suitable values of the TCM's parameters that have been used in the solar convection zone are adopted to make an exploratory application in two stars of 2 and $5M_\odot$ at the RGB and AGB phases. In practical calculations the TCM has been applied to the whole convective envelope including the overshooting regions. When analyzing the characteristics of the turbulent correlations, we separate the whole convective envelope into the convective unstable zone and the convective overshooting region. In the convective unstable zone, we find an approximation approach to explicitly associate the turbulent correlations, which can be used to explain the turbulent properties. Later, we make a comparison between the results of the TCM and those of the MLT about the velocity profile of turbulence and influence on stellar structure and evolution. These obtained features of convective motion by the TCM are highly sensitive to the TCM's parameters. The main conclusions are summarized as follows:

(1) The non-local effect of the turbulent convection is only significantly exhibited around the boundaries of the convective unstable zone, especially around the upper boundary, which is in agreement with the results of Li & Yang (2007). The three correlations $\sqrt{k}$, $\overline{u_r'T'}$ and $\overline{T'^2}$ are nearly peaked at the same place in the convective unstable zone for the same set of TCM's parameters. This is because all of them are directly correlated to a function of $(\nabla - \nabla_{\rm ad})\overline{T}$.

(2) For a fixed heat flux (closely related by $\overline{u_r'T'}$) transferred by the convective motion, compared to the results of the MLT, the TCM will result in a larger turbulent velocity and thus more

violent convective motion. Furthermore, for nearly the same profile of the convection velocity obtained by adjusting the value of the mixing length parameter α for both the TCM and MLT, the superadiabatic convection zone will be extended much farther inward for the TCM than for the case of the MLT and the stellar models based on the TCM will have lower effective temperature.

(3) For the stellar models located up along the Hayashi line, we find that the convective motions become progressively stronger. However, the e-folding lengths of $\sqrt{k}$ in both the top and bottom overshooting regions decrease as the stellar model is located higher along the Hayashi line. The overshooting length of $\overline{u_r' T'}$ is found to be shorter than other turbulent quantities for the same set of TCM's parameters in both overshooting regions, which is consistent with the results of Deng & Xiong (2008) and Zhang & Li (2009). The overshooting distances of $\overline{u_r' T'}$ in the bottom overshooting region are almost the same for different stellar models with the same set of TCM's parameters. Therefore, the bottom convective overshooting has a similar effect on the stellar structure for all of the considered stellar models.

(4) The diffusive parameter $C_{\rm s}$ plays an important role in the development of the isotropic turbulence in the top overshooting region, and a longer isotropic turbulence will be obtained for larger values of $C_{\rm s}$. In the bottom overshooting region, the convection becomes progressively more horizontally dominated for larger values of $C_{\rm s}$, and the convection shows a much more complicated behavior when $C_{\rm s}$ is sufficiently small.

(5) The decaying modes of the turbulent kinetic energy k are very similar for different stellar models based on the same set of TCM's parameters. We find that there is a nearly linear relation between $\lg k$ and $\ln P$ in most of the overshooting regions. The slope of the decaying law seems to be only a function of the TCM's parameters. The values of $C_{\rm s}$ and α have a similar effect on the decaying distance of the turbulent kinetic energy, and the larger their values become, the smaller the slope of the decaying law becomes and therefore the linearly decaying distance becomes longer.

Acknowledgements This work is in part supported by the National Natural Science Foundation of China (Grant Nos. 10973035 and 10673030) and by the Knowledge Innovation Key Program of the Chinese Academy of Sciences under Grant No. KJCX2-YW-T24. Fruitful discussions with Q.-S. Zhang, C.-Y. Ding and J. Su are highly appreciated.

References

Alexander, D. R., & Ferguson, J. W. 1994, ApJ, 437, 879
Bahcall, J. N., Pinsonneault, M. H., & Wasserburg, G. J. 1995, Reviews of Modern Physics, 67, 781
Baker, N. H., & Kuhfuss, R. 1987, A&A, 185, 117
Böhm-Vitense, E. 1953, ZAp, 32, 135
Böhm-Vitense, E. 1958, ZAp, 46, 108
Bressan, A. G., Bertelli, G., & Chiosi, C. 1981, A&A, 102, 25
Busso, M., Wasserburg, G. J., Nollett, K. M., & Calandra, A. 2007, ApJ, 671, 802
Canuto, V. M. 1992, ApJ, 392, 218
Canuto, V. M. 1993, ApJ, 416, 331
Canuto, V. M. 1994, ApJ, 428, 729
Canuto, V. M. 1997, ApJ, 482, 827
Canuto, V. M., & Dubovikov, M. 1998, ApJ, 493, 834
Canuto, V. M., Goldman, I., & Mazzitelli, I. 1996, ApJ, 473, 550
Canuto, V. M., & Mazzitelli, I. 1991, ApJ, 370, 295
Castellani, V., Chieffi, A., Tornambe, A., & Pulone, L. 1985, ApJ, 296, 204
Castellani, V., Giannone, P., & Renzini, A. 1971, Ap&SS, 10, 340
Charbonnel, C. 1995, ApJ, 453, L41

Deng, L., & Xiong, D. R. 2008, MNRAS, 386, 1979
Deng, L.-C., & Xiong, D.-R. 2001, ChJAA (Chin. J. Astron. Astrophys.), 1, 50
Freytag, B., Ludwig, H.-G., & Steffen, M. 1996, A&A, 313, 497
Gratton, R., Sneden, C., & Carretta, E. 2004, ARA&A, 42, 385
Gratton, R. G., Sneden, C., Carretta, E., & Bragaglia, A. 2000, A&A, 354, 169
Herwig, F. 2005, ARA&A, 43, 435
Herwig, F., Bloecker, T., Schoenberner, D., & El Eid, M. 1997, A&A, 324, L81
Hollowell, D., & Iben, I., Jr. 1988, ApJ, 333, L25
Hossain, M. S., & Rodi, W., 1982, Turbulent Buoyant Jets and Plumes, ed. W. Rodi (Oxford: Pergamon Press), 121
Iben, I., Jr. 1975, ApJ, 196, 525
Iben, I., Jr. 1977, ApJ, 217, 788
Iben, I., Jr. 1981, ApJ, 246, 278
Iglesias, C. A., & Rogers, F. J. 1996, ApJ, 464, 943
Jiang, S. Y., & Huang, R. Q. 1997, A&A, 317, 121
Kraft, R. P., Sneden, C., Langer, G. E., & Shetrone, M. D. 1993, AJ, 106, 1490
Lattanzio, J. C. 1989, ApJ, 344, L25
Li, Y., & Yang, J.-Y. 2001, ChJAA (Chin. J. Astron. Astrophys.), 1, 66
Li, Y., & Yang, J. Y. 2007, MNRAS, 375, 388
Maeder, A. 1975, A&A, 40, 303
Pedersen, B. B., Vandenberg, D. A., & Irwin, A. W. 1990, ApJ, 352, 279
Pilachowski, C. A., Sneden, C., & Booth, J. 1993, ApJ, 407, 699
Ramírez, S. V., & Cohen, J. G. 2002, AJ, 123, 3277
Recio-Blanco, A., & de Laverny, P. 2007, A&A, 461, L13
Renzini, A. 1987, A&A, 188, 49
Rogers, F. J. 1994, in IAU Colloq. 147: The Equation of State in Astrophysics, eds. G. Chabrier & E. Schatzman (Cambridge: Cambridge Univ. Press), 16
Rogers, F. J., & Iglesias, C. A. 1995, in Astrophysical Applications of Powerful New Databases, Astronomical Society of the Pacific Conference Series, 78, eds. S. J. Adelman & W. L. Wiese, 31
Rogers, F. J., Swenson, F. J., & Iglesias, C. A. 1996, ApJ, 456, 902
Sackmann, I.-J. 1980, ApJ, 241, L37
Salasnich, B., Bressan, A., & Chiosi, C. 1999, A&A, 342, 131
Saslaw, W. C., & Schwarzschild, M. 1965, ApJ, 142, 1468
Spruit, H. C., Nordlund, A., & Title, A. M. 1990, ARA&A, 28, 263
Sreenivasan, S. R., & Wilson, W. J. F. 1978, Ap&SS, 53, 193
Straniero, O., Chieffi, A., Limongi, M., et al. 1997, ApJ, 478, 332
Ulrich, R. K. 1970, Ap&SS, 7, 183
Ventura, P., & D'Antona, F. 2005, A&A, 431, 279
Xiong, D.-R. 1979, Acta Astronomica Sinica, 20, 238
Xiong, D.-R. 1981, Scientia Sinica, 24, 1406
Xiong, D. R. 1985, A&A, 150, 133
Xiong, D.-R. 1990, A&A, 232, 31
Xiong, D.-R., Cheng, Q. L., & Deng, L. 1997, ApJS, 108, 529
Yang, J. Y., & Li, Y. 2007, MNRAS, 375, 403
Zhang, Q.-S., & Li, Y. 2009, RAA (Research in Astronomy and Astrophysics), 9, 585